NASA CONTRACTOR REPORT

NASA CR-1300

NASA CR-1300 c. l

STUDY OF LOW PRESSURE APPLICATION OF NEW ORBITRON AND ION GAUGE DESIGNS

by Charles M. Gosselin

Prepared by
MIDWEST RESEARCH INSTITUTE
Kansas City, Mo.
for Langley Research Center

NATIONAL AERONAUTICS AND SPACE ADMINISTRATION • WASHINGTON, D. C. • JUNE 1969

NASA CR-1300

STUDY OF LOW PRESSURE APPLICATION OF NEW

ORBITRON AND ION GAUGE DESIGNS

By Charles M. Gosselin

NATIONAL AERONAUTICS AND SPACE ADMINISTRATION

PREFACE

The ultimate goal of this program has been to study ways by which the orbitron gauging technique can be applied to extremely low pressure measurements. The program, which has been supported by NASA under Contract No. NAS1-7458, was monitored by Mr. Alphonsa Smith of the NASA - Langley Research Center. This report describes the research accomplished during the period 19 June 1967 - 18 September 1968.

The program was conducted in the Physics Branch of Midwest Research Institute under the direction of Mr. Gordon Gross, Manager of the Branch, and Mr. Charles Gosselin, Project Leader. Mr. S. K. Behal, who was on a sabbatical leave from the Central Scientific Instrument Organization, Chandigarh, India, contributed to the program during his six-week (February - March 1968) visit to Midwest Research Institute.

TABLE OF CONTENTS

TABLE OF CONTENTS (Concluded)

List of Figures

STUDY OF LOW PRESSURE APPLICATION OF NEW
ORBITRON AND ION GAUGE DESIGNS

by Charles M. Gosselin
Midwest Research Institute

ABSTRACT

Three experimental orbitron gauges have been designed and fabricated. These gauges have been designed so as to use the technique of reduced ion-collector area which was introduced by Bayard and Alpert and the technique of suppression of photoemission from the ion collection introduced by Schuman. The basic concepts of uhv measurements and a basic model of or-bitron gauge operation are reviewed. Also fabrication techniques are de-scribed. Pressure response curves are displayed. The combination of the suppressor grid with the orbitron gauge appear to offer significant promise for operation below 10^{-11} torr. A second type gauge was also studied viz. the "buried collector" gauge. A pressure response curve is also displayed for this device.

I. INTRODUCTION

A. Vacuum Measurement

Any measurement requires some interaction between the measuring device and that which is to be measured. The resulting effect (the "signal") produced by such an interaction can then be used to characterize the physical parameter which is to be described. Of course, the usefulness of any "signal" is directly related to (1) the ability of the observer or his instruments to establish accurate correlations between the "signal" and the parameter which is to be described and (2) the ability to discern real "signals" from spurious signals.

The measurement of the level of evacuation becomes a particularly difficult task in the very low gas density realm (below 10^{-10} torr). As higher levels of evacuation are achieved there are smaller quantities of gas with which to interact and therefore the "signal" is very small.

The ordinary means employed in vacuum gauges to interact with low density gas environments is electron bombardment. Such bombardment of gas produces positive ions which can be collected and counted (via appropriate electrodes and electrometers). It has been demonstrated many times that the ion current can be related to the gas density; therefore,

the ion current is a useful "signal" resulting from the interaction between residual gas and the bombarding electrons.

However, the problems associated with uhv measurements include not only the detection of the ion current "signal" but also the discrimination of the real signal (resulting from the electron bombardment of the environmental gas which is to be measured) from spurious "signals." Most spurious signals encountered in uhv gauging are associated with the generation and trapping of the electrons.

This discussion will be restricted to gauges which are based on dependent discharge* techniques. In such gauges thermionic emission is usually employed to generate controlled quantities of electrons. These electrons are accelerated to an energy level sufficient to cause gas ionization ($\sim$ 125 eV) and as they travel through the gauge ionizing collisions occur which generate the ion "signal." The electrons are ultimately collected at the accelerating electrode (anode). However, because of the high energy of the electrons when colliding with the anode, low energy x-radiation is emitted. The intensity of this radiation depends on the density and energy of electrons falling on the anode. Photoemission produced from the ion collecting electrode by the x-radiation constitutes a spurious "signal." The level of this spurious "signal" is controlled by the radiation intensity and the gauge geometry. Ultraviolet radiation can also generate spurious "signals".

Adsorbed gas can be ejected from the anode either as neutral molecules or ions by electron bombardment. (See ref. 1.) These desorbed products are representative of the surface environment rather than the gas environment and spurious "signals" can be generated by their ionization and collection.

Other spurious signals can be generated by leakage currents across insulators, inductive coupling, and electronic equipment noise.

In the development of dependent discharge vacuum gauges several significant techniques have been employed to reduce the spurious "signal" to real "signal" ratio. Bayard and Alpert (ref. 2) reduced the area of the ion collector in their "inverted trode" gauge. Schuemann (ref. 3) used suppression of the photoemission from the ion collector in his "suppressor grid" gauge. Mourad et al. (ref. 4) used electrostatic entrapment to extend electron paths in the orbitron gauge. Each of these concepts has resulted in improved operation or offers significant promise for gauge development. Although

---

* A dependent discharge requires an external source of electrons to sustain a discharge or current flow. For example a hot filament provides this source in a Bayard-Alpert Gauge.

there are other important developments to the general field of vacuum measurement which could be reviewed, they do not lie within the area of techniques studied under the present project.

B. Purpose of This Study

The purpose of the study reported here is to determine if the ratio of spurious "signal" to ion "signal" can be reduced in an orbitron type gauge by decreasing the area of the ion collector and by the suppression of photo-emission.

Three experimental gauges have been constructed for this study. Each gauge design incorporates one or more of the techniques described above. The design and fabrication techniques for each gauge are described in Section II of this report. The response of the experimental gauges are found in Section IV.

One additional experimental gauge, viz., the Buried Collector Gauge (ref. 5) has been briefly studied. This gauge which has been developed at NASA's Langley Research Center was loaned to MRI for this study. Its response characteristics are given in Section V.

C. Methods

The ability to evaluate gauge response in the very low pressure range is necessary if the limiting effect of spurious signals is to be determined. For this study, therefore, a dynamic pressure ratio technique has been employed.

The pressure ratio technique is outlined schematically in Figure 1. A steady flow of a test gas is established from a gas inlet system through a restricted conductance into a uhv pumping station. The pressure (P_t) at the test gauge is determined by the equation:

$$P_t = \frac{Q}{S}$$

where: Q = a steady flow rate of a test gas through the pressure ratio system, and

S = pumping speed of the uhv system for the test gas. The pressure at the reference gauge (P_r) is

```
                    ┌─────────────────────────────┐
              ──────►   DUAL CHANNEL RECORDER   ◄──────
              │     └─────────────────────────────┘     │
       ┌──────┴──────┐   ┌───────────────┐   ┌──────────┴──┐
       │  REFERENCE  ├───┤ CONDUCTANCE(C)├───┤    TEST     │
       │    GAUGE    │   └───────────────┘   │    GAUGE    │
       └──────┬──────┘                       └──────┬──────┘
       ┌──────┴──────┐                       ┌──────┴──────┐
       │  TEST  GAS  │                       │  UHV PUMP   │
       │ SOURCE  (Q) │                       │ STATION (S) │
       └─────────────┘                       └─────────────┘
```
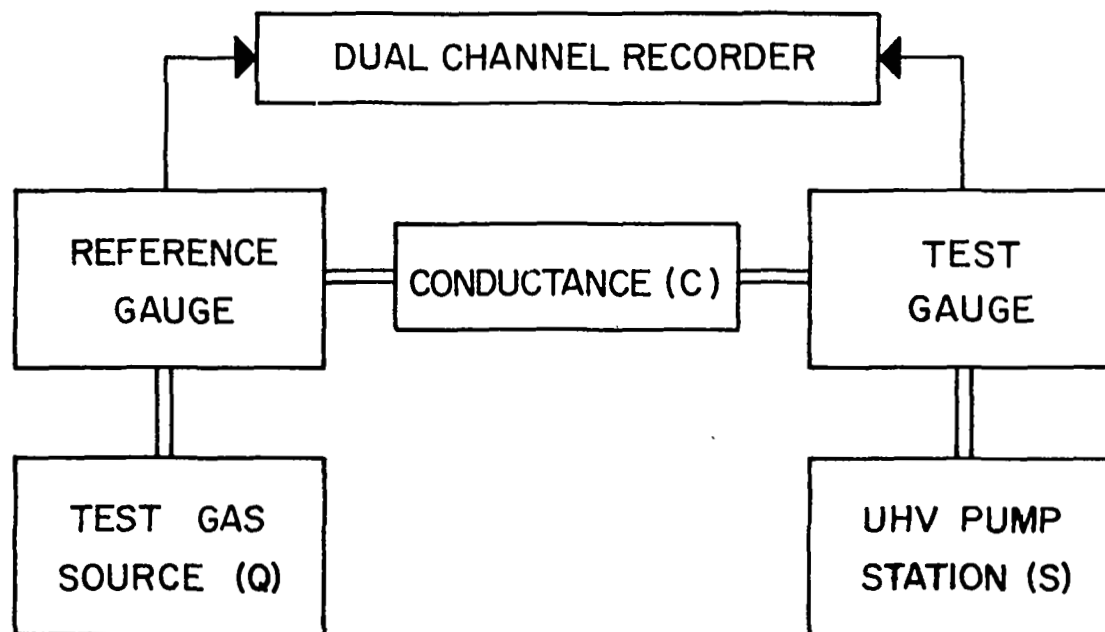
Figure 1 - Diagram of Pressure Ratio Technique. The flow (Q) of a test gas through the conductance
(C) establishes a pressure ratio between the reference gauge and test gauge positions.
This relationship can be used to determine the pressure in the test volume (P_t) by
measurements of pressure in the reference volume (P_r) as long as; (1) P_T is controlled
by equilibrium flow conditions; (2) C remains constant, and (3) the pumping speed for
the test gas (S) remains constant.

$$P_r = \frac{Q(C + S)}{SC} \quad ,$$

where: C = conductance between the test position and the reference position. The pressure ratio between the test and reference gauge positions is given by

$$\frac{P_t}{P_r} = \frac{C}{C + S} = K \; .$$

If C and S are constant, then K is constant and

$$P_t = KP_r \; .$$

Therefore, the pressure at the test gauge position can be determined by measuring the pressure at the reference gauge position, if the following requirements are maintained: (1) a steady flow of a test gas is established, (2) the conductance between the upstream (reference) position and downstream (test) position does not change, and (3) a constant pumping speed for the test gas is maintained by the uhv system. Implied in this technique are the requirements that the background pressure is small compared with the flow regulated pressure P_t and that there are no other sources or sinks for the test gas between the two chambers.

The dynamic pressure-ratio method is described by Knudsen's equations. (See ref. 6.) The main requirement, to insure the validity of this method for pressure comparisons, is to maintain a constant conductance orifice across which pressure differences are maintained. The application of the dynamic pressure-ratio method to gauge calibration was discussed at the 1961 Washington meeting of the American Vacuum Society. Florescu (ref. 7) described the advantages of the two-calibrated conductance method and possible modifications to account for gauge desorption and pumping limitations. Roehrig and Simons (ref. 8) described a large system with orifice limited pumps which provided pressure calculation to 10^{-9} torr. Actually, the leak-up method of Dushman and Found (ref. 9) and the application of pressure-ratio techniques to mass spectrometer sampling (ref. 10) indicates that this basic technique has long been known and applied. This method has been employed successfully to determine response characteristics for cold cathode gauges over their complete operating range (down to 2.5×10^{-12} torr) (see refs. 11, 12). The uhv pressure ratio system is described in the Equipment section of this report.

II. ORBITRON GAUGES

A. Description of Orbitron Gauge Operation

The orbitron gauge and the normal controls and power supplies needed to operate it are shown diagrammatically in Figure 2. The gauge consists essentially of two coaxial cylindrical electrodes and an electron insertion electrode. The center cylindrical electrode (anode) is maintained at a high positive potential and the outer cylindrical electrode (cathode) is maintained at ground potential. The cathode is split into two parts, each of which is electrically isolated. The upper part is used as the ion collector and is connected through an electrometer to ground. The lower part of the cathode is connected directly to ground and is used to establish the proper field conditions around the electron insertion electrode. It is not connected to the electrometer because of the high level of spurious signals which are collected in this region of the cathode.

The electron insertion electrode is mounted between the anode and lower cathode and is maintained at a potential which is lower than the surrounding field points thus producing local perturbations in the cylindrical field. This electrode consists of a fine tungsten wire (0.001 in. dia.) suspended between two support posts. By thermionic emission, electrons are generated from the tungsten wire and are accelerated into the cylindrical electrostatic central field between the anode and cathode. Due to field perturbation about the insertion electrode, and the orientation of the tungsten wire with respect to the support posts, the electrons are injected into the electrostatic central field with a desired tangential component of velocity. As a result, the electrons are placed in open elliptical orbits about the anode and remain entrapped in these orbits until they gain enough energy to collide with the cathode or lose enough angular momentum to collide with the anode. Electron energy changes can occur because of electron-electron, electron-molecule, or electron-filament interactions.

The electrons encounter a reflecting field at each end of the cylindrical electrodes and therefore reverse their axial velocity component. Entrapped in the gauge volume the electrons make many orbits before they are ultimately lost. Because of the electrons' long path length fewer electrons are needed to maintain a desired electron density, and the number of electrons falling onto the anode is proportionally reduced. Resultant x-ray generation, molecular desorption, and ionic desorption in the orbitron are generally less than in a standard Bayard Alpert Gauge (BAG) operating at the same electron density. However, unlike the BAG, the ion collector of the orbitron subtends a very large solid angle about the anode and therefore is quite efficient in detecting most of the x-ray generation that does occur. Although the orbitron collector is ~ 100 times as efficient in detecting the x-ray generation
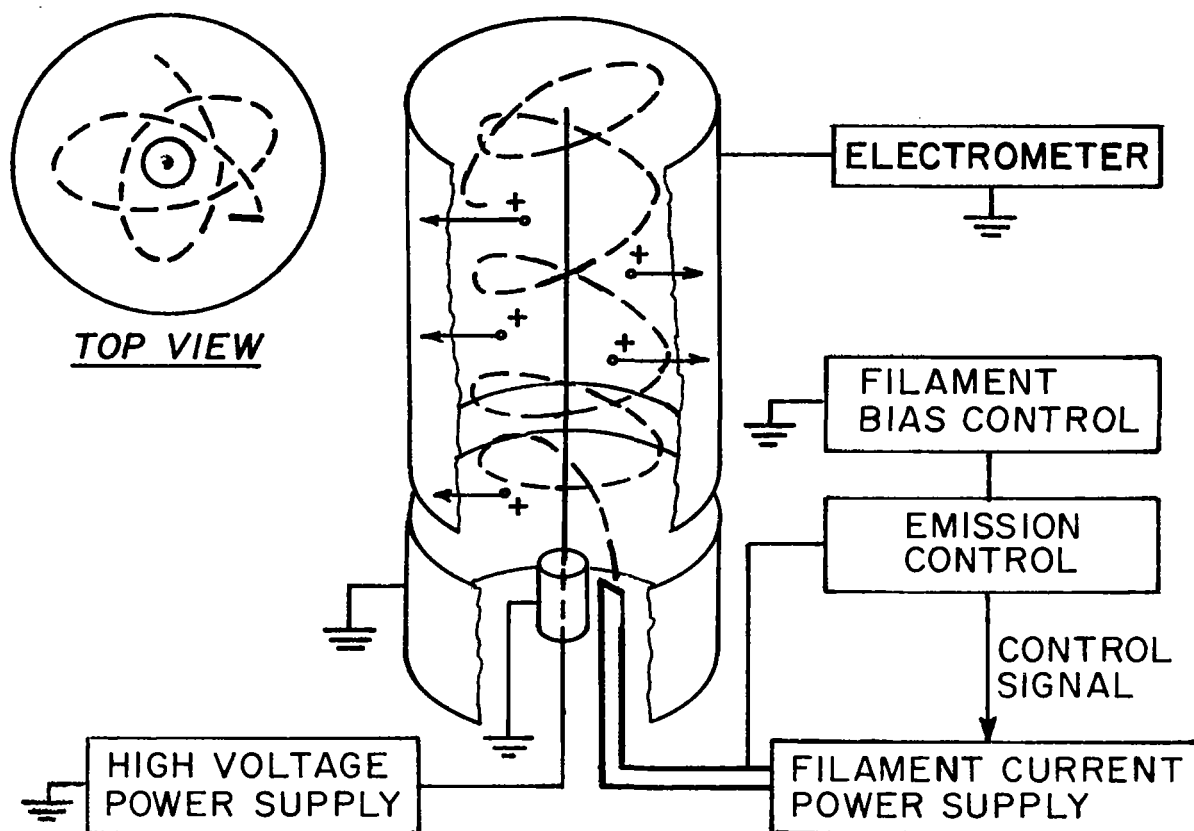
TOP VIEW

Figure 2 - Diagram of Orbitron and Major Electronic Components. Electrons
    emitted from the filament orbit the center electrode and
    generate ions by collisions with gas molecules. The ions
    are collected by the upper portion of the split cylindrical
    electrode.

as a BAG, the number of electrons falling onto the anode is less by a factor of $\sim 10^{-3}$. Therefore, in comparison with the BAG a standard orbitron should exhibit a lower spurious "signal" to ion "signal" ratio by a factor of ~ 10.

B. Experimental Orbitron Gauges

Three experimental orbitron gauges have been designed, constructed, and tested on this program. They are (1) the Control Orbitron Gauge (COG), (2) the Reduced Area Ion Collector Orbitron Gauge (RAICOG), and (3) the Suppressor Grid Orbitron Gauge (SGOG).

1. <u>Control orbitron gauge</u>.-- The control orbitron gauge (COG) is shown in Figure 3. The gauge is mounted on a 4-1/2 in. O.D. Con Flat flange into which a nine pin electrical feedthrough has been welded. Three 1/8 in. O.D. x 1-1/4 in. long stainless steel support posts have been welded to the flange on a 1-15/16 in. dia. circle at 120° intervals. To each of these posts a 1/8 in. O.D. x 8 in. long ceramic* rod has been attached via a set screw coupler. The various electrodes of the gauge have been designed and fabricated such that they are supported by the three ceramic rods.

The cathode assembly has been fabricated from two sections of 1-1/2 in. O.D. thin walled (0.010 in.) stainless steel tubing (type 304). At each end of each cathode section a stainless steel support ring is attached and is used to connect the cathode section to the three ceramic support rods. The upper section (ion collector) is 5 in. long and the lower section is 7/8 in. long. They are separated and electrically isolated by ceramic* spacers (1/4 in. O.D. x 1/8 in. I.D. x 1/8 in. thick) threaded onto the three ceramic support rods.

The anode is a 0.005 in. dia. tantalum wire and is attached at one end to the center electrical feedthrough in the flange and at the other end to a spring loading assembly. Figure 4 shows the spring loading assembly. It is electrically connected not only to the anode but also to one of the electrical feedthroughs via a ceramic tube clad wire. The spring assembly unit consists of a stainless steel spider support unit, a tungsten helical spring, and an anode wire clamp. Tungsten was chosen as the spring material because it must maintain mechanical strength at bakeout temperatures up to 400°C. The primary purpose for the spring mounting is to eliminate anode distortions during high temperature ($\sim 900°C$) anode degassing. Degassing of the anode is accomplished by passing ~ 425 mA through the anode. This procedure removes adsorbed gas from the anode surface thus reducing desorption sources for spurious signals.

---

* McDanel AP-35 High Density Ceramic.

Figure 3 - Control Orbitron Gauge (COG). The cathodes are mounted on three ceramic rods. Location of the elements is estab-lished by 1/8 in. thick ceramic spacers threaded onto the ceramic support rods.
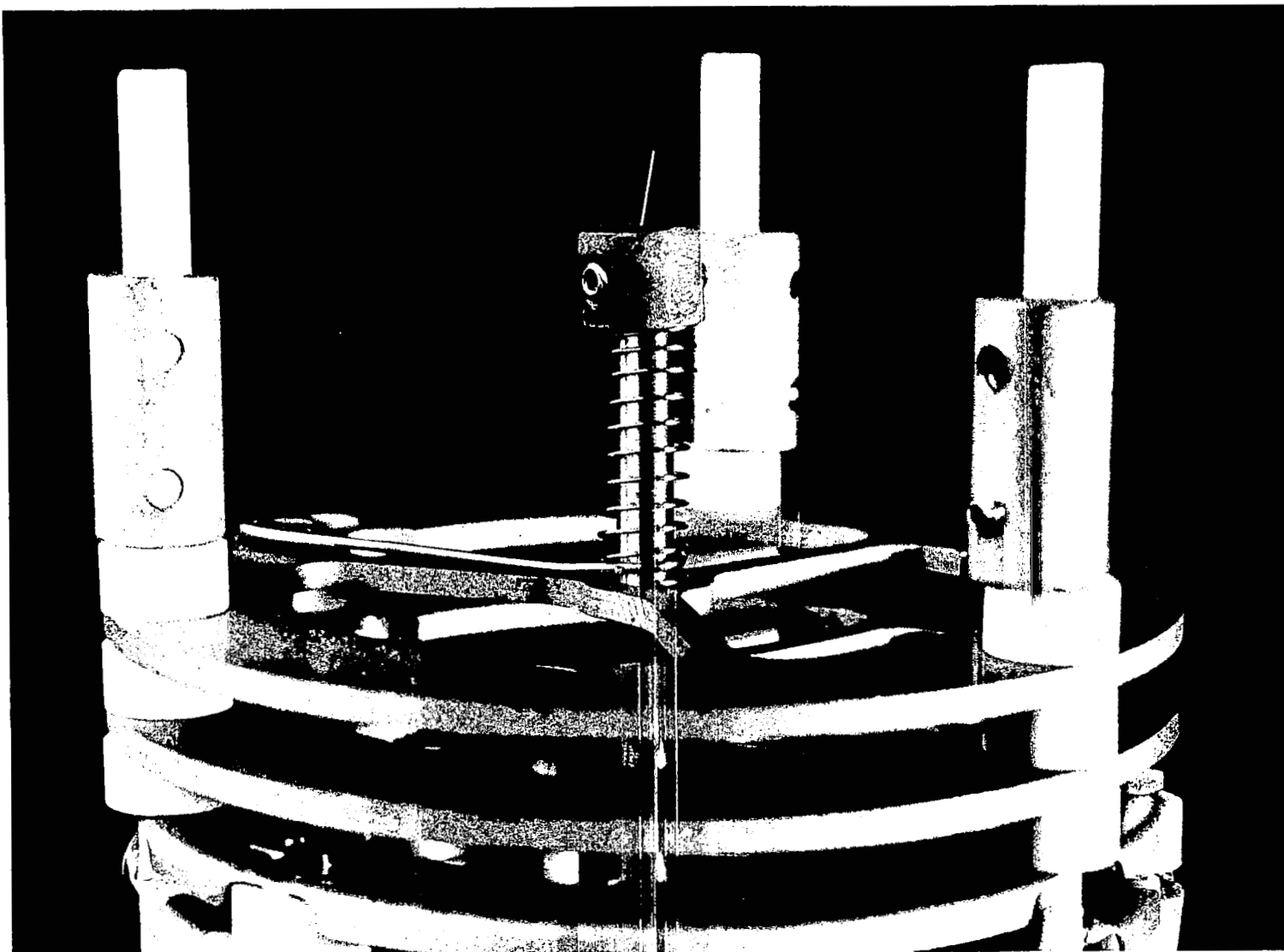
Figure 4 - Spring Loading Anode Support Assembly. The 0.005 in. dia. anode passes out of the electron orbiting region through a 1/8 in. O.D. x 0.010 in. (wall thickness) x 1/2 in. long tube and is attached to a circular clamp. This clamp is spring loaded by means of a tungsten helical spring.

At each end of the cathode the anode passes through a 1/8 in. O.D. thin walled (0.010 in.) stainless steel tube which is mounted on spider assemblies similar to that used for the spring assembly above. These tubes are positioned so as to establish a reflecting electric field for the orbiting electrons. The upper tube (adjacent to the spring assembly) extends into the cathode volume 1/2 in. and the lower tube (adjacent to flange) extends into the cathode volume 1 in. The lower spider assembly also acts as the filament support as shown in Figure 5.

The filament support design permits the filament to be operated at one of three radial positions within the gauge, viz., 0.3, 0.5, and 0.7 of the cathode radius (1-1/2 in.). The filament can be inserted into or withdrawn from the electron orbiting region (as defined by the lower reflector tube). This design also permits the filament to be rotated about an axis parallel to the anode at the three radial positions mentioned above. Once the filament height and the angular adjustments are made, its position can be fixed by the locking screw in the support ring.

For the operational test conducted on this study, the filament was located in the radial position closest to the anode (0.3). The height position of the 1/8 in. long thoriated tungsten filament was between the planes defined by the gap separating the cathode sections. The filament was rotated 45° from a radial line defined by the anode and the filament axis of rotation.

2. Reduced area ion collector orbitron gauge.-- The reduced area ion collector gauge (RAICOG) is shown in Figure 6. The unique feature of this gauge is that the ion collector is a helical coil. This design reduces significantly the solid angle subtended by the ion collector from the anode, thus reducing photo generated background current. However, in order to improve the efficiency of ion collection, an outer helical coil is positioned around the ion collector so that an electrical field can be established which will trap and focus ions onto the inner coil (the ion collector). The focusing field is established by maintaining the ion collector at ground potential and establishing a positive potential on the repeller grid (outer coil).

The design and construction of this gauge is identical to the COG with the exception of the ion collector and ion focusing grid assembly. This assembly consists of (1) two helical coils, the ion collector 1-1/2 in. dia. x 4-7/8 in. long and the ion focusing coil 1-7/8 in. dia. x 4-3/4 in. long; and (2) a support ring assembly. The support ring assembly is made up of two support rings rigidly fixed 5 in. apart by three 1/8 in. dia. ceramic spacers and by 1/16 in. dia. bolts. The outer coil is attached to the ceramic spacers of the support ring assembly. The inner coil (ion collector) is attached to an additional set of 1/16 in. dia. ceramic tubes which are also attached to the support rings. The latter tubes are long enough to pass through a set of holes in the support rings of the lower cathode and are used as conduits

AXIS OF ROTATION

FILAMENT

FIXED REFLECTOR TUBE

FILAMENT MOUNTING UNIT

SUPPORT RING
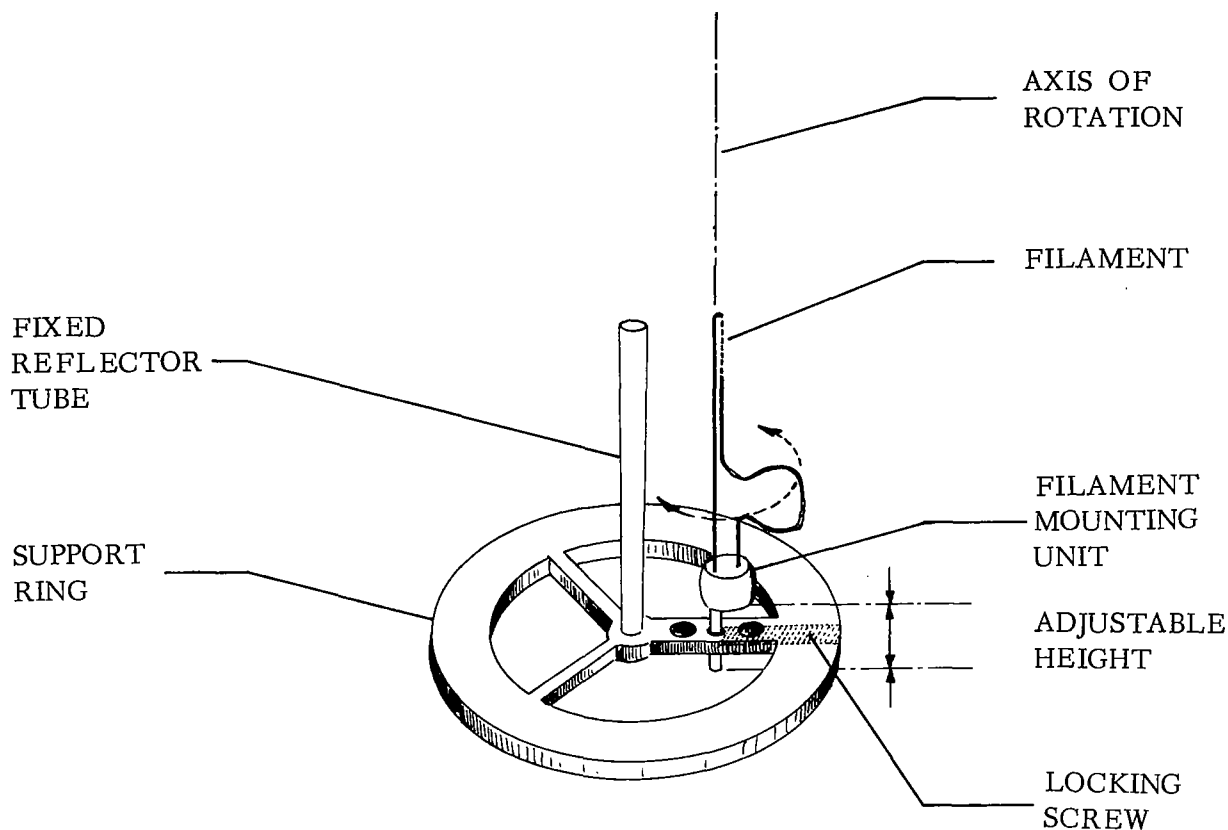
ADJUSTABLE HEIGHT

LOCKING SCREW

Figure 5 - Reflector Tube and Filament Mount for Orbitron Gauge. The filament mounting unit can be located at three radial positions, viz., 0.3, 0.5, and 0.7 of the cathode radius. The unit can also be translated into or withdrawn from the orbiting discharge region and rotated about an axis parallel to the anode at each of the radial positions (see Figure 10).
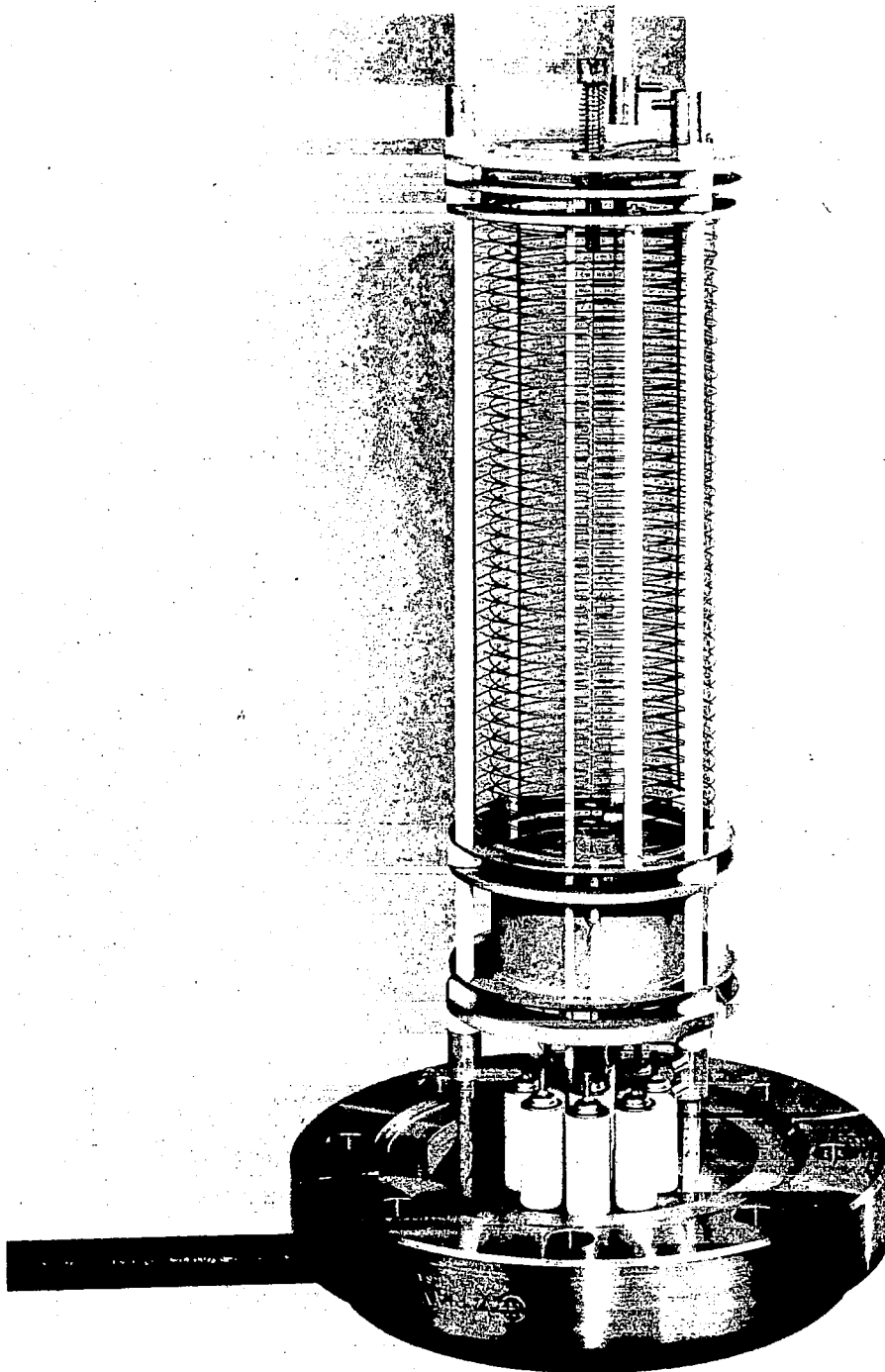
Figure 6 - Reduced Area Ion Collector Orbitron Gauge with Ion Focusing
Grid (RAICOG). The outer helical coil is used to focus
ion onto the inner helical coil (ion collector).

for electrical wires to the flange. The entire assembly is mounted on the main 1/8 in. dia. ceramic support rods described in section Bl above.

3. _Suppressor grid orbitron gauge._ -- The suppressor grid orbitron gauge (SGOG) is shown in Figure 7. The unique characteristic of this gauge is that a 1-1/2 in. dia. helical coil electrode separates the 1-7/8 in. dia. solid ion collector from the electron orbiting volume. The helical coil is maintained at a negative potential with respect to the ion collector and therefore acts as a suppressor grid for secondary emission from the ion collector. Since the helical coil is part of the electron orbiting volume the other electrodes defining this volume (viz., the lower cathode and both reflector tubes) are also maintained at the suppressor grid potential. The ion collector is connected via an electrometer to ground.

Both the helical coil and the ion collector are mounted in a support ring assembly similar to that described for the RAICOG. However, a guard ring electrode has been added at each end of the ion collector. These electrodes are held in position by sets of ceramic insulators. Silver paint has been used to provide a conducting ring around each ceramic rod to shunt any leakage currents to the guard ring electrode. The guard ring unit is maintained at the same potential as the ion collector and therefore shields the ion collector from leakage currents.

The helical coil is mounted on three 1/16 in. dia. ceramic tubes which are mounted in the support ring assembly as described for the RAICOG. The ion collector is positioned within the ceramic support columns by ceramic spacers. All other design parameters of this gauge are identical to the COG and RAICOG.

C. Fabrication Technique for Orbitron Gauges

The fabrication of parts for the experimental gauges has required the development of several special tools and techniques. Among these special tools have been an inexpensive stamping die and drill jig for fabrication of the support ring. Figure 8 shows a stainless steel ring blank, the die assembly, the drill jig, and a finished part.

Special mandrels were fabricated from plexiglass rods and copper bars for construction of the tantalum grid coils used in the RAICOG and the SGOG. Figure 9 shows two mandrels which have been made; one for the 1-1/2 in. O.D. coils and one for the 1-7/8 in. O.D. coils. After the tantalum wire (0.010 in.) is wound on the coils, a stainless steel rod is spot welded to each wire where it crosses each of three copper strips. During the spot welding process the copper strips are used as electrodes. Upon completion of the operation the center portion of the mandrel is removed as well as the copper strips.
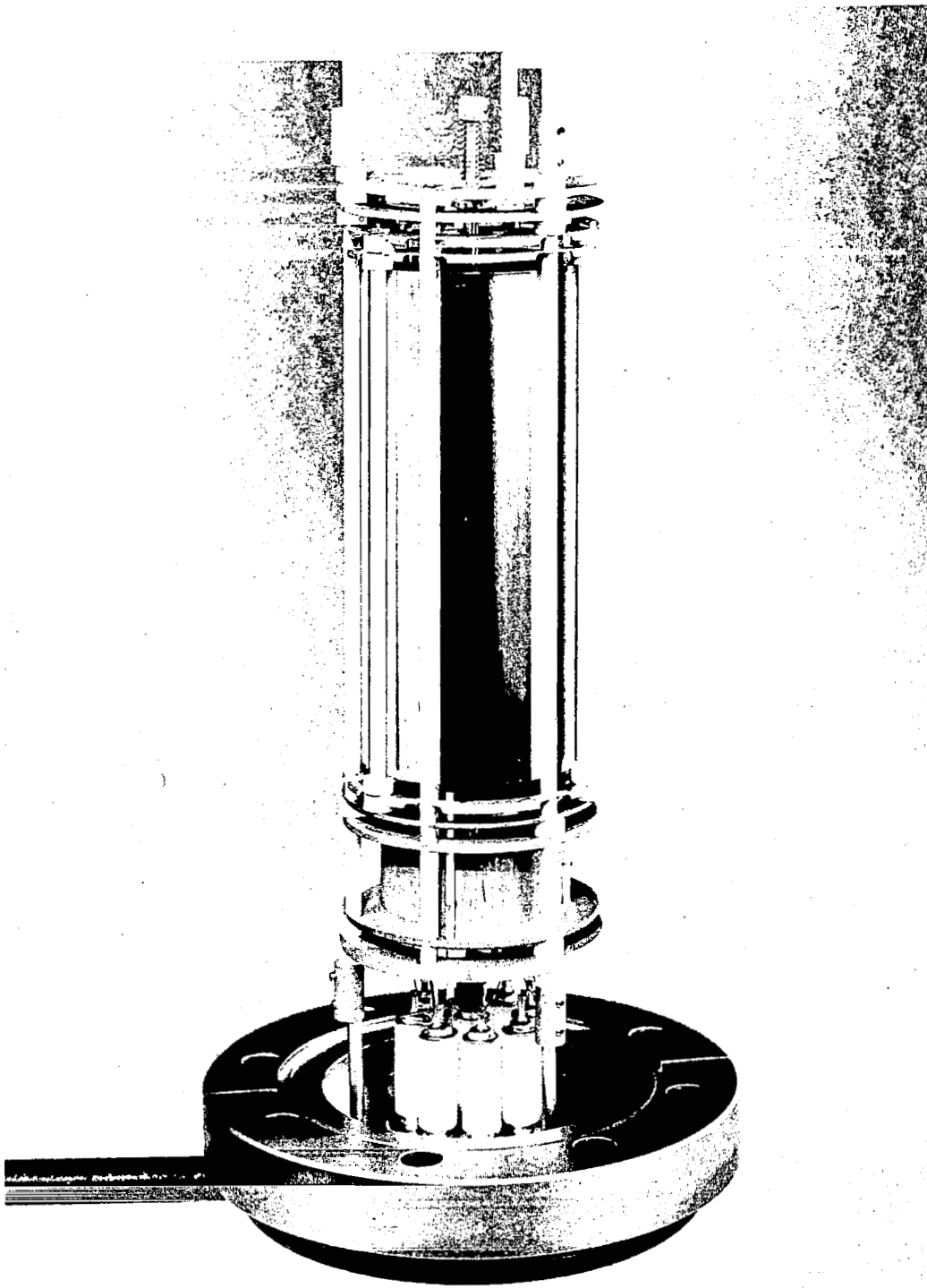
14

Figure 7 - Suppressor Grid Orbitron Gauge. An inner helical coil is
used to suppress secondary electron emission from the
solid cylindrical ion collector. Also guard ring elec-
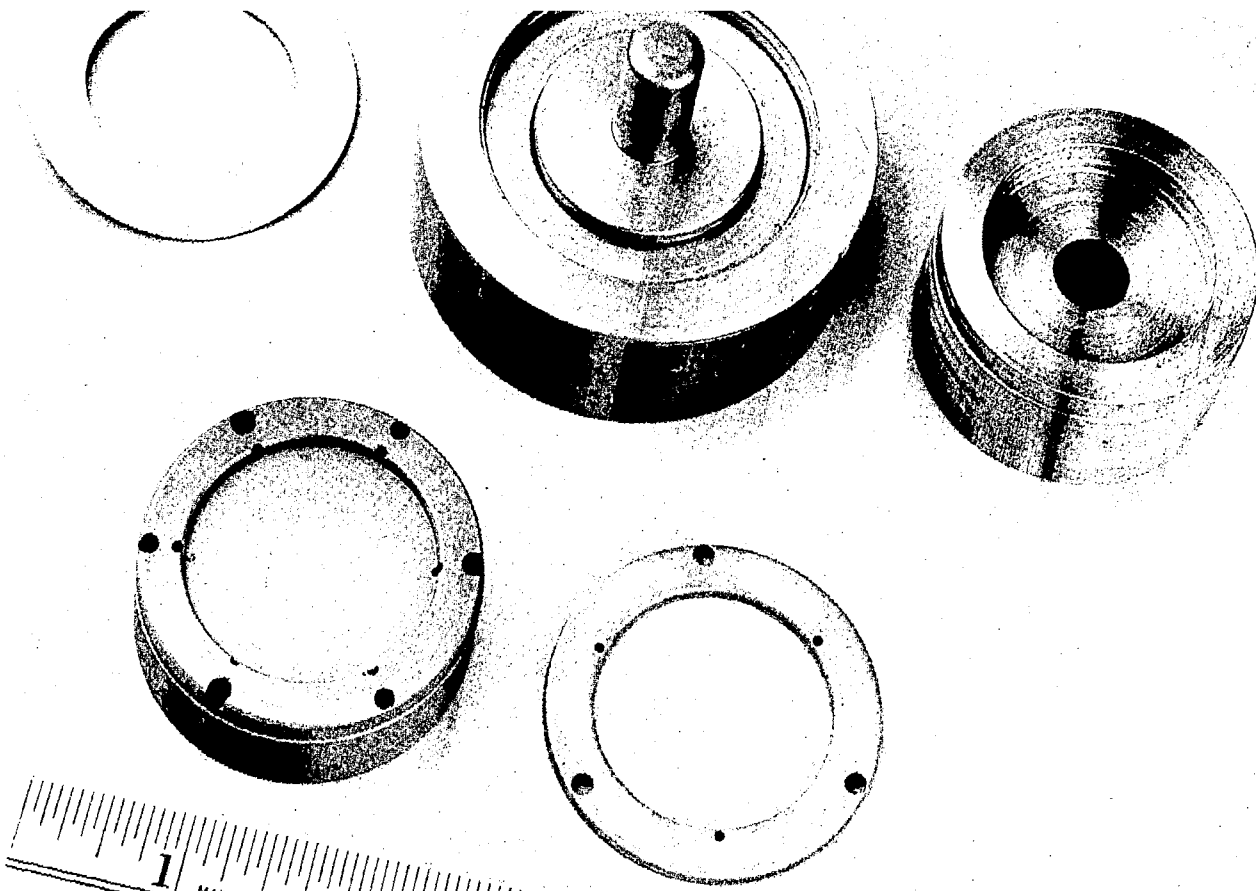trodes are used to shield the ion collector.

Figure 8 - Stamping Die and Drill Jig Used to Fabricate Support Ring Units. Stainless Steel blanks (0.015 in. thick) are precut and stamped. Required holes are drilled using a simple jig (lower left). Finished support ring shown at lower right.
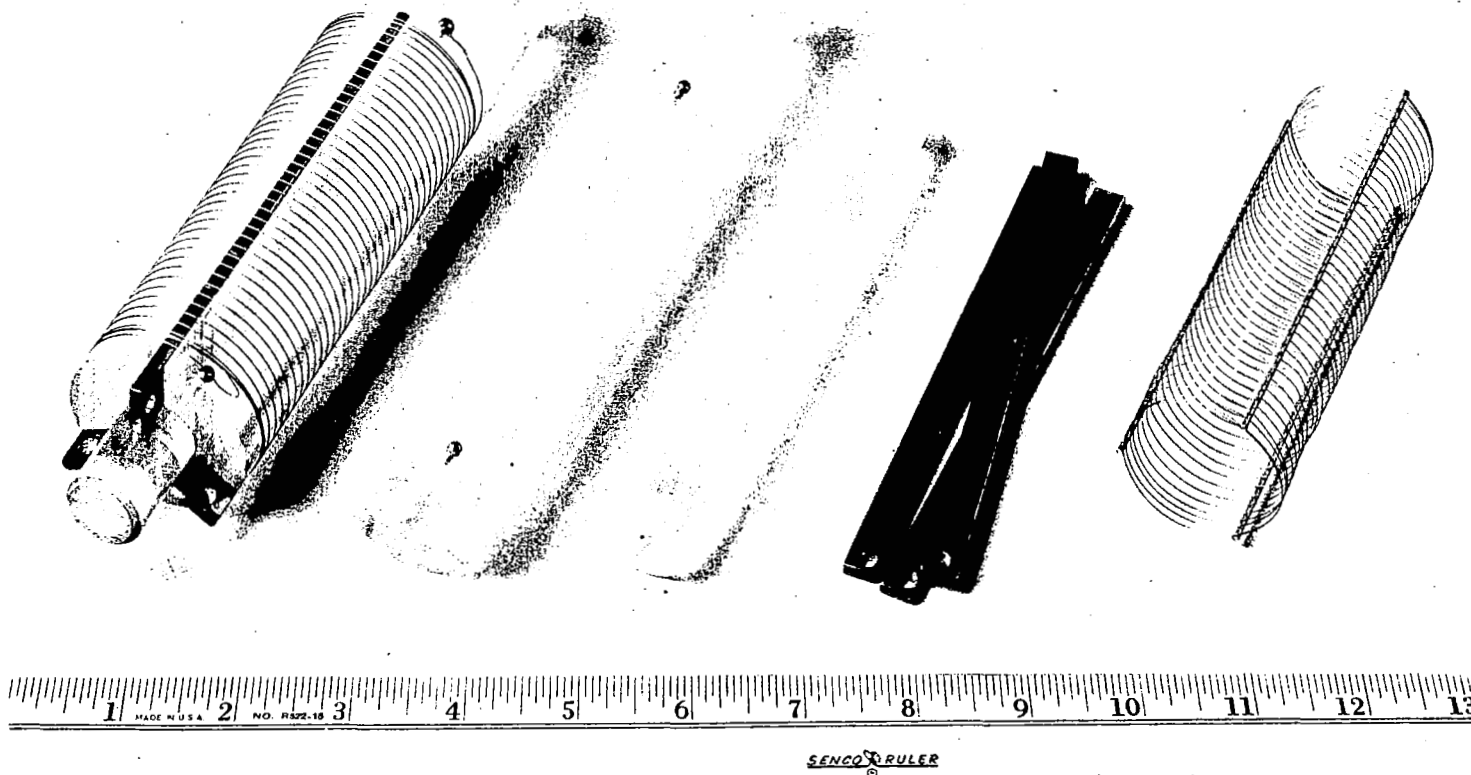
Figure 9 - Plexiglas Winding Mandrels for Fabrication of Helical Coils. Tantalum wire (0.010 in. dia.) is wound onto one of the mandrels. The coils are held in position permanently by spot welding three stainless steel rods to each turn of the coil at 120° intervals.

Removal of these parts produces a reduction in the outside diameter of the mandrel, thus permitting removal of a coil assembly which is also shown in Figure 9.

The filament mounting unit is shown in Figure 10. It consists of a 1/2 in. dia. x 1/8 in. thick glass disk into which a 1/16 in. dia. Kovar support post and two 0.040 in. dia. Kovar filament support posts have been embedded. A 0.005 in. tantalum wire is spot welded to each of the 0.040 in. dia. posts. The tantalum wire which is on axis with the 1/16 in. dia. support post is pulled straight and plastically deformed so as to make it rigid. A small hook is made at the loose end. The other tantalum wire is formed into a single loop spring with a straight shank adjacent to the other tantalum wire. This shank is cut off at a point 3/16 in. below the hook described above and a 0.001 in. dia. thoria-doped tungsten wire is spot welded to the loose end. The tungsten wire is then stretched across the gap between the tantalum wires and spot welded to the hook area of the other tantalum wire. As the tungsten wire is pulled the gap between the tantalum wires is closed to 1/8 in. before the welding operation is carried out. The distance between the tungsten wire and the adjacent parallel tantalum wire should be 1/32 in. or less.

III.   VACUUM TEST EQUIPMENT

The uhv pressure ratio system is shown schematically in Figure 11 and photographically in Figure 12.

The primary design features of a uhv pressure-ratio system are twofold: (1) the system must be capable of maintaining a sufficiently low background pressure so that known flow conditions will control the pressure value (P_t) at the test gauge position and (2) the system must be equipped with a suitable gas inlet subsystem including a constant value conductance between the test and reference chambers.

Special design criteria and operating techniques are employed to insure a low background pressure level. The methods employed are: (1) the entire pressure ratio system is bakeable to 400°C, (2) large area titanium sublimation pumps (TSP) are located in both the upstream (reference) and downstream (test) volumes, (3) the system can be cooled to liquid nitrogen temperature, thus reducing desorption and increasing the pumping speed of the TSPs, and (4) the reference gauges are carefully outgassed by long term filament operation and electron bombardment of metal gauge parts.

The test gas used for operation of the pressure ratio system is helium. This gas is chosen since it can be easily admitted into a uhv system via a vycor diffuser.
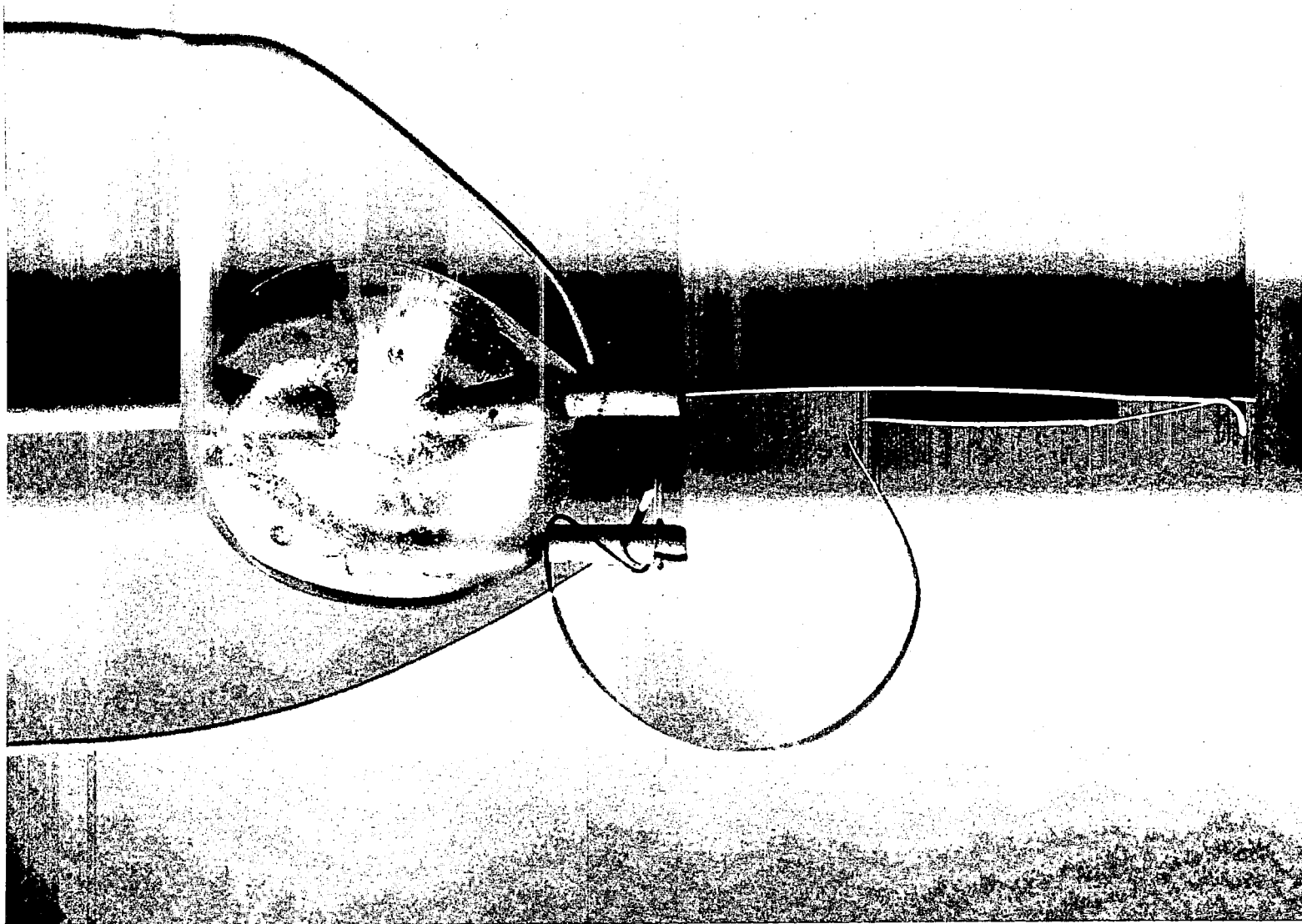
Figure 10 - Filament Mounting Unit. A tungsten filament (0.001 in. dia.) is mounted between two 0.005 in. dia. tantalum support rods. The support on the right has been shaped into a single loop spring in order to maintain tension on the filament.

TO AUXILIARY PUMPING STATION

ISOLATION VALVE I

REFERENCE GAUGE I

REFFERENCE VOLUME & TSP I

GAS INLET SYSTEM

ISOLATION VALVE II

TEST VOLUME

ADJUSTABLE CONDUCTANE (C)

TEST GAUGE

REFERENCE GAUGE II

TSP II

LHe CRYOPUMP (S)

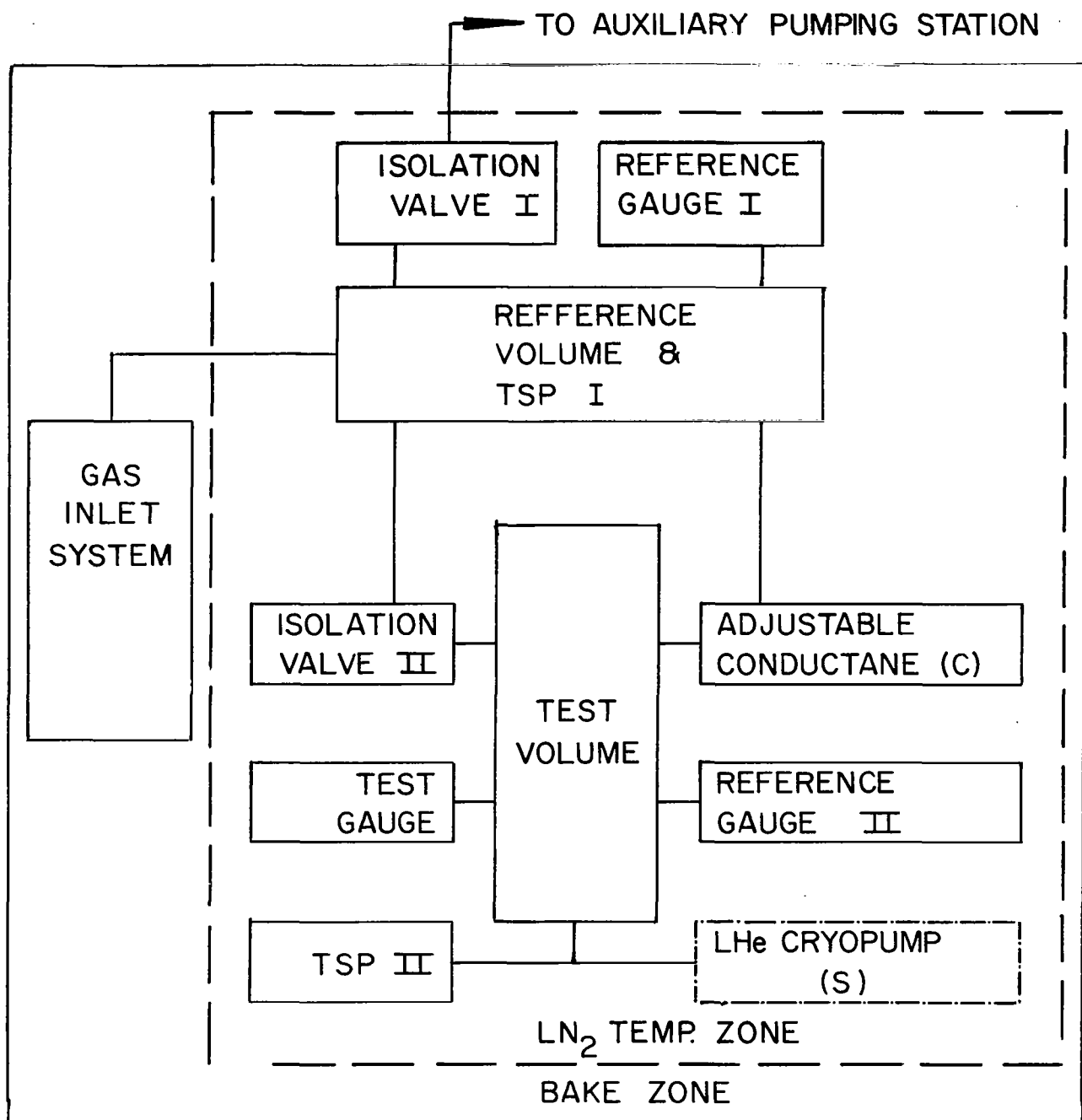LN_2 TEMP. ZONE

BAKE ZONE

Figure 11 - Block Diagram of the UHV Pressure Ratio System. The background in the system is maintained at a low level by (1) reduced desorption resulting from cooling uhv surfaces to LN_2 temperature following 400°C bake, and (2) high pumping speed of titanium sublimation pumps (TSP) for active gases.
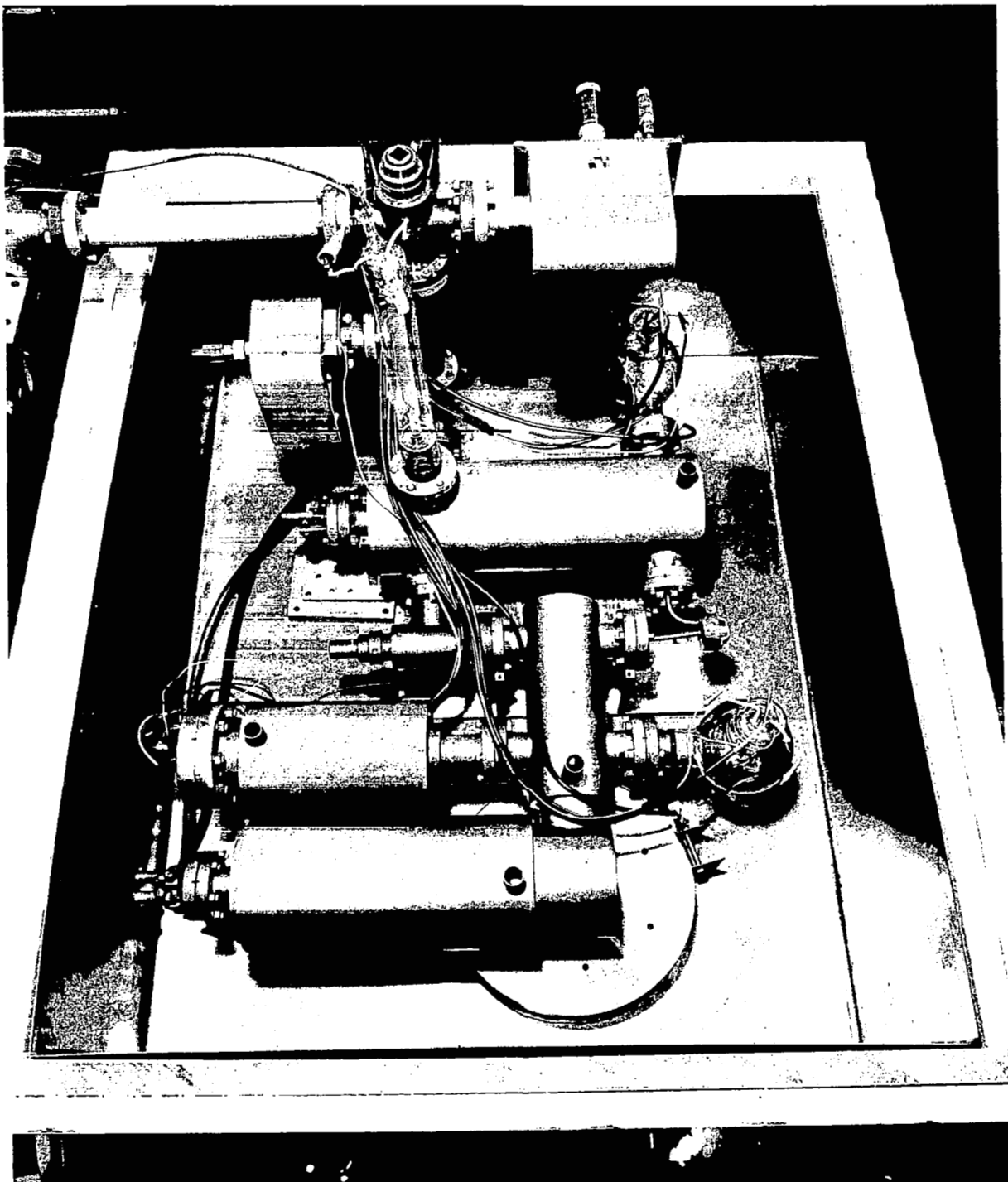
Figure 12 - UHV Pressure Ratio System. The pressure ratio system is mounted within an insulated stainless steel tank. During low pressure tests LN_2 is circulated through the doubled walled vacuum vessels and exhausted into the stainless steel tank.

The He gas is further purified of active gas species such as H_2 and CO as it passes through TSP-I. The TSPs have no effect on He gas even when operated at liquid nitrogen temperature.

The adjustable conductance between the reference and test volumes is a Granville-Phillips variable leak valve. When the valve is full open, a pressure ratio $\frac{P_t}{P_r} = 1.4 \times 10^{-3}$ can be maintained when the liquid helium cryopump is activated. To insure that the ratio does not change during a run, the conductance (c) is held constant by establishing a constant equilibrium system temperature before a test is begun and by maintaining this condition throughout the test period. The pumping speed for the test gas is maintained constant by the use of a conductance limited LHe cryopump.

The pressure ratio is verified for each run by direct B-A gauge reading at the reference gauge positions. These measurements are made at pressure levels well above the residual current limitation of the B-A gauges. The B-A reference gauges have been calibrated through the 10^{-9} range via the pressure ratio technique and the pressure reference transfer technique. (See ref. 13.)

The reference volume, TSP-I, test volume, and TSP-II are double walled, such that liquid nitrogen can be circulated in the enclosed space. After passing through the double walled region the LN_2 is exhausted into a liquid tight insulated box which surrounds the pressure ratio system (see Figure 12). Evaporation of the puddling LN_2 on the floor of the box provides a cold N_2 gas environment in which to conduct the pressure ratio study. The insulated box also provides a furnace environment for bakeouts up to $400°C$.

Figure 13 displays the stainless steel test chamber into which the test orbitrons are mounted. The chamber is equipped with a double wall around the test region through which liquid nitrogen can flow during a test. The chamber can be attached to an existing uhv system via a 2-3/4 in. O.D. rotatable Con Flat flange.

IV. RESPONSE OF THE EXPERIMENTAL ORBITRON GAUGES

A. Data

Two types of data have been collected in order to establish the response characteristics of the experimental orbitron gauges, viz., comparison to reference gauges by both direct and pressure ratio techniques.

The gauge response data are presented in terms of the ion collector current in amperes vs. the pressure in torr nitrogen equivalent units. Although
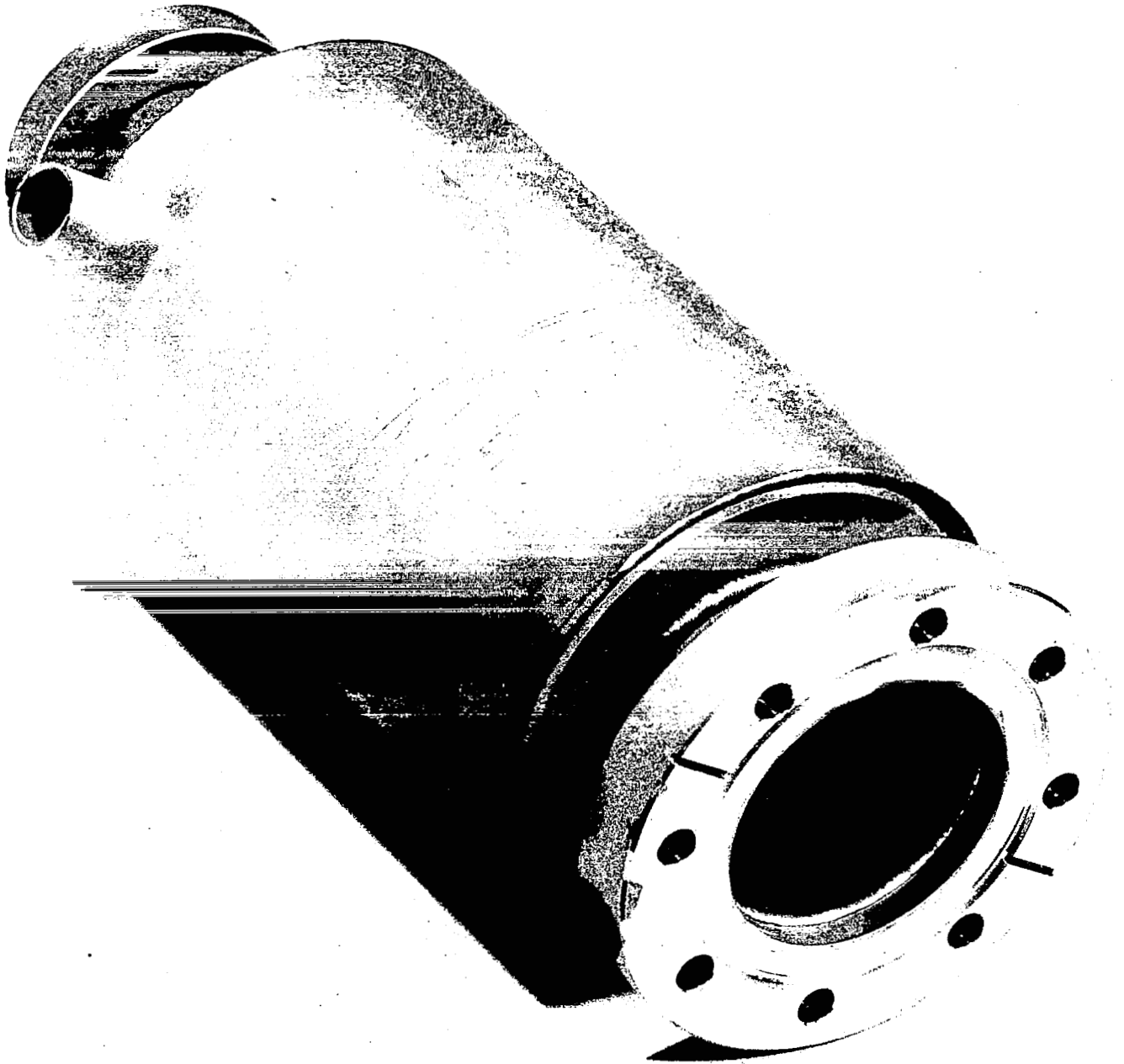
Figure 13 - Test Chamber for Orbitron Gauges. The chamber is fabricated from
        stainless steel and is equipped with a double wall. LN_2 is
        circulated through the double walled region during ultra low
        pressure tests.

the test gas used in this study was helium, the data were converted to torr nitrogen equivalent units by applying the simple relation

$$P_{N_2} = \frac{S_{He}}{S_{N_2}} P_{He}$$

where: S_{He} = sensitivity of the reference gauge for helium

S_{N_2} = sensitivity of the reference gauge for nitrogen

P_{He} = pressure of helium

The value of S_{He}/S_{N_2} used in this work was 0.16.

The pressure ratio technique is used primarily to determine the low pressure response characteristics whereas the direct comparison is used to determine the higher pressure characteristics.

The operating parameters used for this study were selected by varying individual parameters around previously established values (ref. 14) so as to obtain a combination of high sensitivity and low background. Although other sets of parameters could be found for which higher sensitivities were obtained, higher background currents were also measured.

Table I lists the operating parameters used for each of the experimental orbitrons. Also a half profile of the potential distribution in a radial plane, which passes through the filament, is given for each gauge. These profiles are based on calculations for cylindrically symmetric electrodes and have been drawn such that the anode represents the center of an electron potential well, i.e., positive voltages increase in the downward direction.
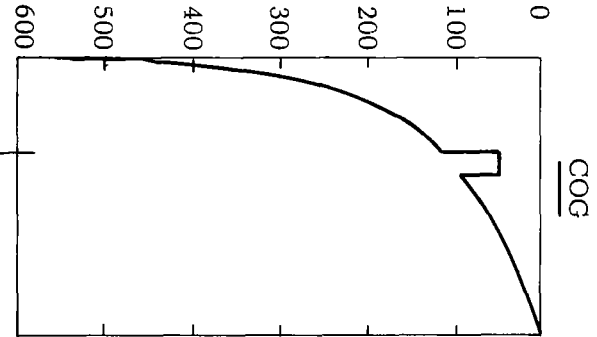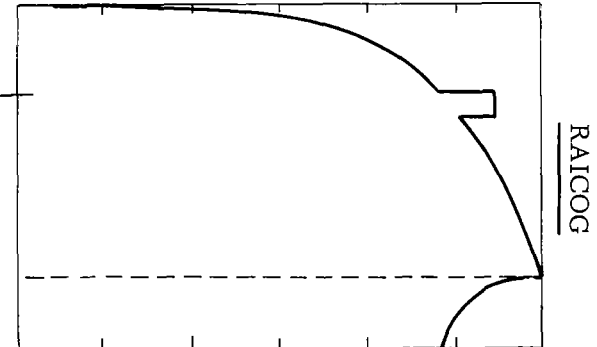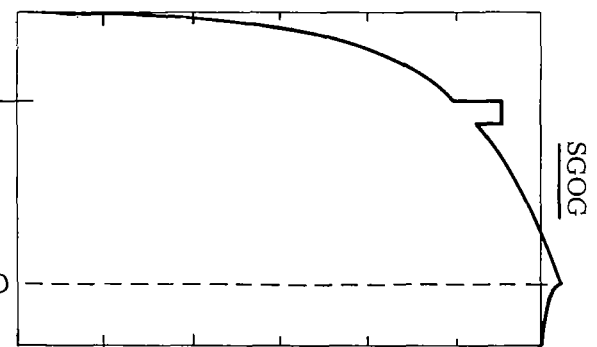
The control orbitron gauge response characteristics for an emission current of 1 μA are shown in Figure 14. A pressure independent ion collector current of $\sim 1.3 \times 10^{-12}$ A was measured in the ultra low pressure range. At higher pressures the gauge responded with a linear slope corresponding to a sensitivity of 0.025 A/torr (N_2).

The reduced area ion collector orbitron gauge response characteristics for an emission of 7 μA are shown in Figure 15. A pressure independent background current of 2.28×10^{-12} A was measured at the ion collector in the ultra low pressure range. The gauge response was studied below this background level by supplying a zero suppression signal of 2.28×10^{-12} A to the electrometer. However, the background was not stable enough to collect reliable data below that which are shown in Figure 15.

24

TABLE I

OPERATING PARAMETERS FOR EXPERIMENTAL ORBITRON GAUGES

	COG	RAICOG	SGOG
VA	+553	+550	+550
Vf	+50	+52.5	+45
V collector	0	0	0
V cathode	0	0	-19
V (Ion repeller)	-	+115	-
V (suppressor grid)	-	-	-19
I_e (Emission)	1 μa	7 μa	7 μa

COG

ANODE FILAMENT ION COLLECTOR

(0, 100, 200, 300, 400, 500, 600)

RAICOG

ANODE FILAMENT ION COLLECTOR ION REPELLER
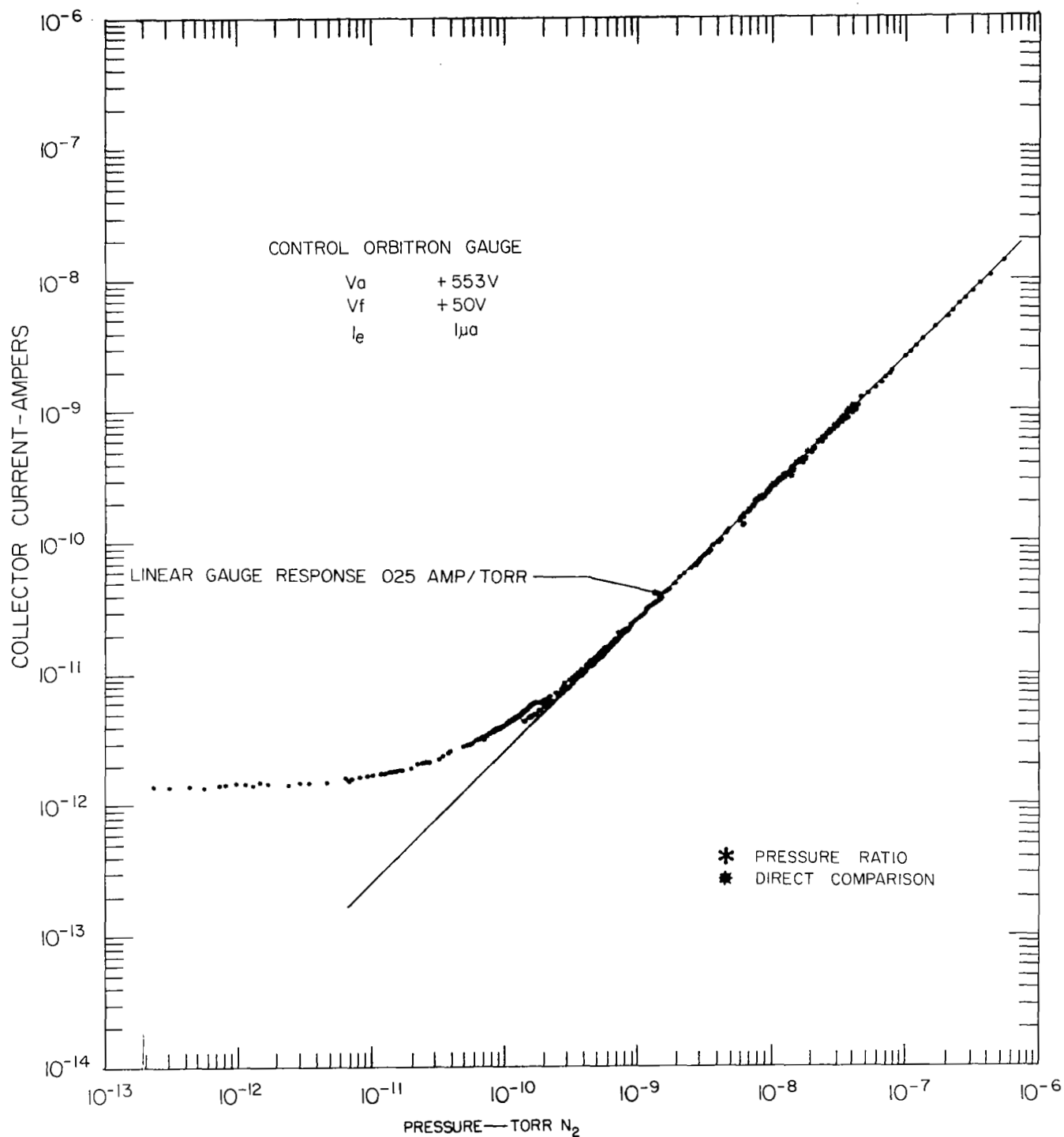
SGOG

ANODE FILAMENT SUPPRESSION GRID ION COLLECTOR

Figure 14 - Control Orbitron Response Curve for 1.0 μA Emission.
Ultra low pressure values plotted on the abscissa
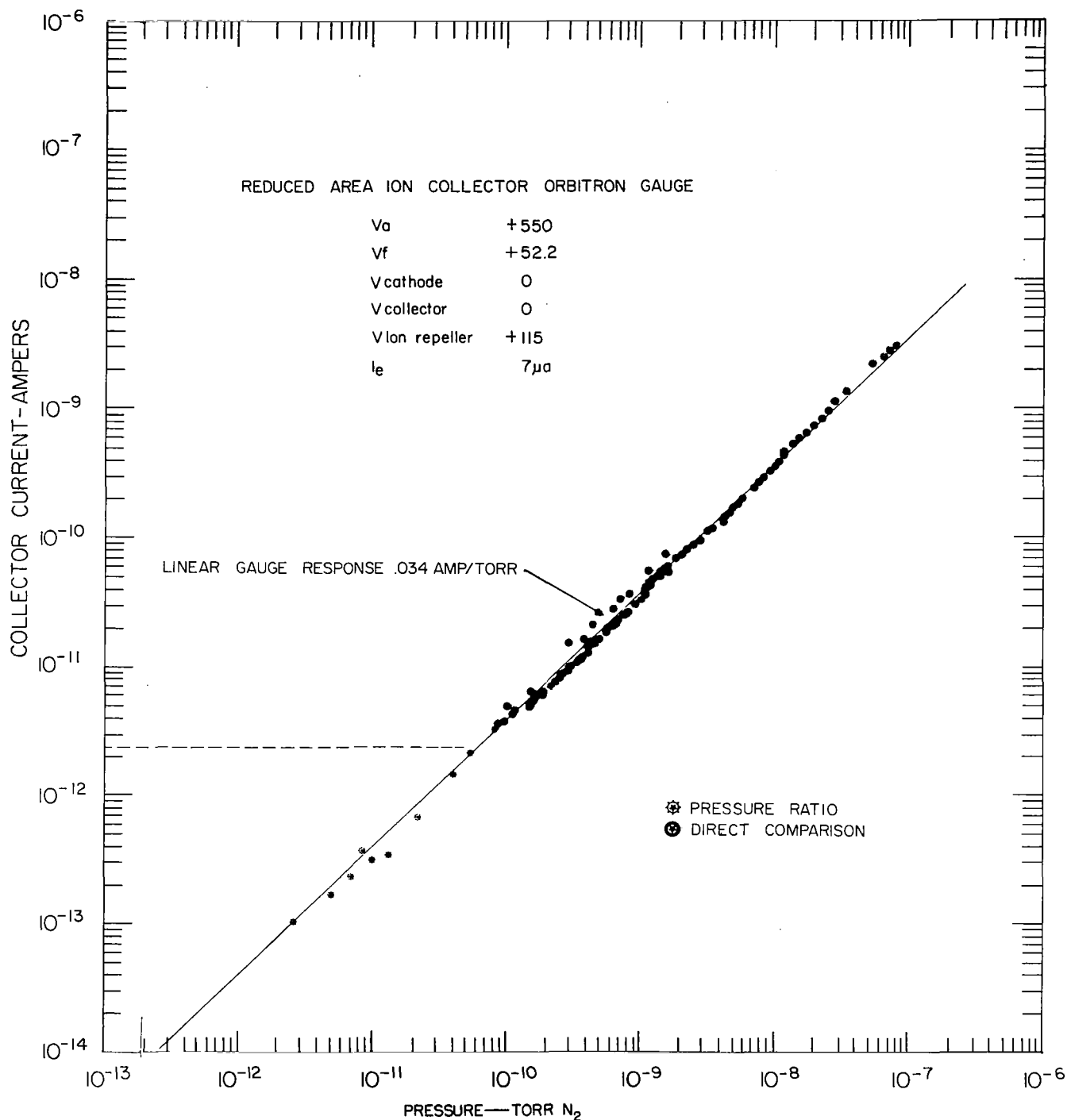were determined by the pressure ratio technique.

Figure 15 - Reduced Area Ion Collector Orbitron Response Curve for 7.0 μA
Emission. Ultra low pressure values plotted on the abscissa
were determined by the pressure ratio technique. The dashed
horizontal line represents the level of a zero suppression
signal which was supplied to the electrometer during the
RAICOG tests.

The data points therefore represent the actual ion collector current less 2.28×10^{-12} A. The gauge response indicated a linear slope corresponding to a sensitivity of 0.34 A/torr (N_2).

The suppressor grid orbitron gauge response characteristics for an emission of 7 μA are shown in Figure 16. The pressure independent background ion collector current in this gauge was negative, viz., -1.07×10^{-12} A. Attempts were made to eliminate the negative background currents by varying the operating parameters but without success as long as the gauge was operated in a suppressor grid mode, i.e., while the electrodes surrounding the electron orbiting volume were operating at a negative potential with respect to the ion collector. The parameters finally chosen which yielded the -1.07×10^{-12} A ion collector background current are listed in Table I. The data points presented in Figure 15 were obtained by plotting the actual current measurement plus the absolute value of the background level, i.e., $I + 1.07 \times 10^{-12}$ A. The data scatter in the low pressure region of the curve are believed to be due to noise in the voltage power supplies used for the anode potential and suppressor grid potential. The SGOG gauge displayed a near linear response corresponding to a sensitivity of $\sim$ 0.076 A/torr (N_2).

Figures 17 and 18 display a comparison of the response of the RAICOG and the SGOG to helium and to hydrogen. This comparison was made on a getter-ion pumped vacuum system in which a Varian uhv-12 was used as a reference gauge for direct comparison. The uhv-12 was compared to the calibrated (for helium) reference gauge on the pressure ratio system and found to read $\sim$ 8% low. The data in the Figures 17 and 18 have, therefore, been adjusted to agree with the reference gauges of the pressure ratio system. Both figures show that the ratio of sensitivities for hydrogen vs. helium (S_{H_2}/S_{He}) is slightly larger for the experimental orbitron gauges than for the uhv-12. This is evidenced by the small but distinct separation between the response curves in Figures 17 and 18 for the two gases.

It is interesting to note that the sensitivity indicated in Figure 17 for the RAICOG is $\sim$ 29% higher than that indicated in Figure 15. Although the same emission current was used for both sets of experiments. The explanation of this discrepancy cannot be simply attributed to the indicated difference in operating potentials. The set of operating potentials used for the data in Figure 17 was also tried when the RAICOG was attached to the uhv pressure ratio system; however, the gauge indicated a sensitivity of $\sim$ 0.01 A/torr. This was only 20% of the sensitivity indicated in Figure 17. An adequate explanation for this behavior has not been determined. The only obvious environmental difference between the two sets of experiments was that the gauge housing (vacuum chamber) used to collect the data for Figure 17 was a dielectric (glass) whereas for Figure 15 it was metal (see Figure 13).
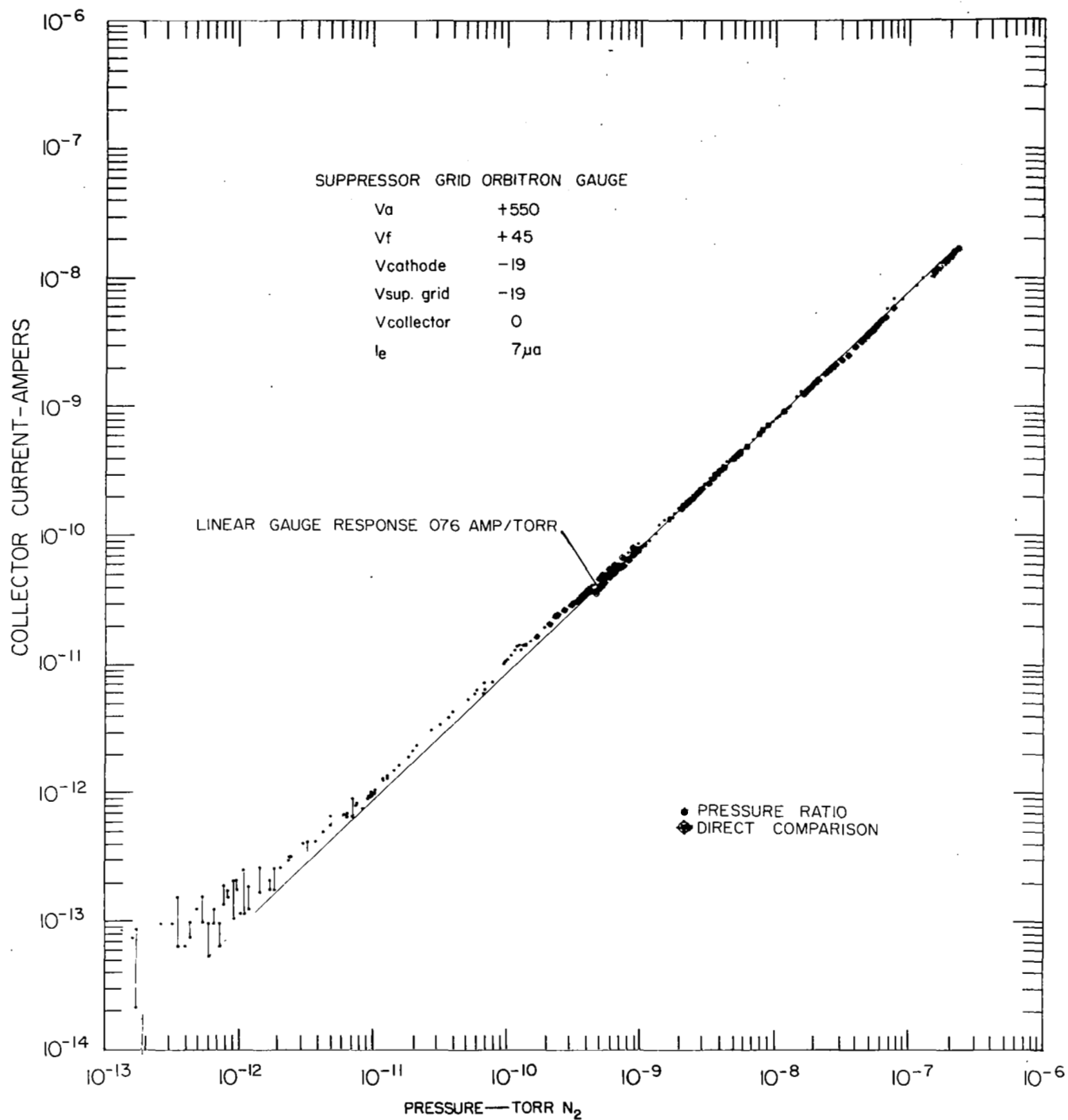
Figure 16 – Suppressor Grid Orbitron Response Curve for 7.0 µA Emission. Ultra low pressure values plotted on the abscissa were determined by the pressure ratio technique.
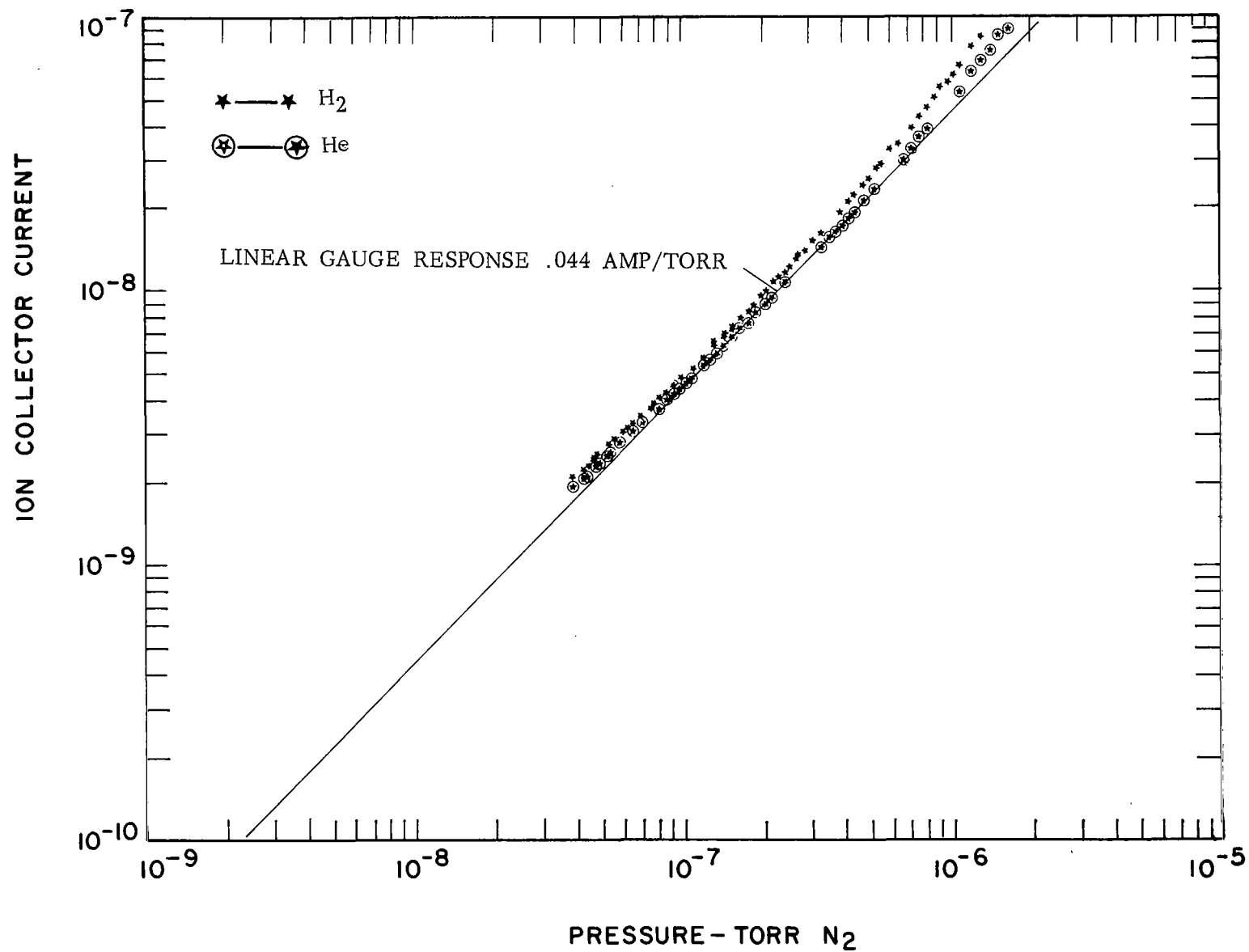
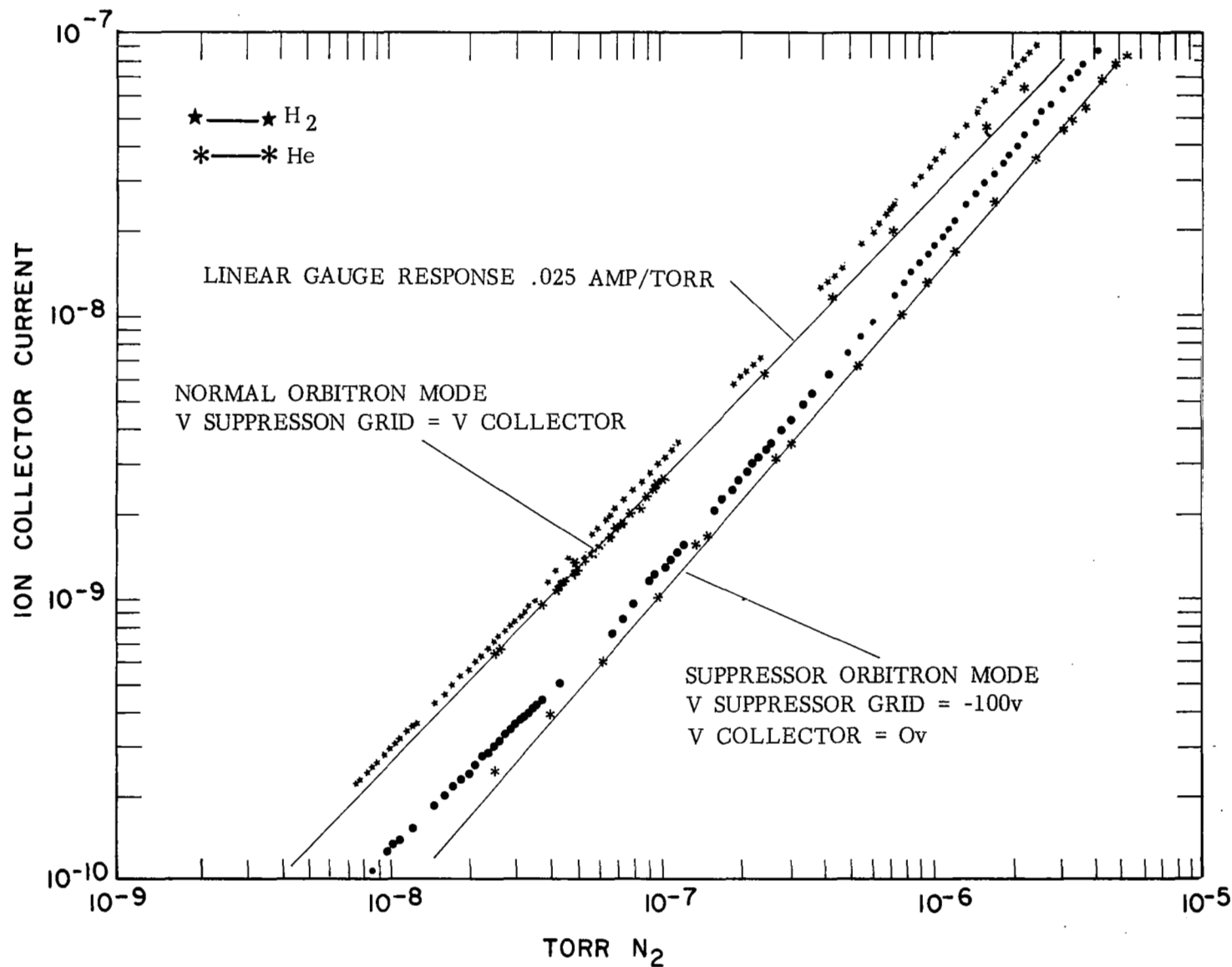Figure 17 - Comparison of the Relative Response of the RAICOG to a UHV-12 for Helium and Hydrogen

Figure 18 - Comparison of the Relative Response of the SGOG to a UHV-12 for Helium and Hydrogen. The SGOG was operated in two modes, i.e., standard orbitron mode similar to the COG (cathode potential equal ion collector potential) and the suppressor mode (cathode potential less than ion collector potential).

The operational parameters used for the RAICOG pressure ratio experiments were re-adjusted to obtain a close to maximum sensitivity condition.

The data in Figure 18 display the response of the SGOG for two modes of operation: (1) for the suppressor grid operating at the collector potential (ground) and (2) for the suppressor grid operating at -100 V and the ion collector operating at ground. The first mode of operation yielded a near linear response for both hydrogen and helium. The response for helium corresponds to a sensitivity of 0.026 A/torr (N_2) for an emission current of 1 µA. This value is in excellent agreement with the curve shown in Figure 14 for the control orbitron gauge. The second mode of operation yielded a nonlinear response corresponding to a slope of approximately 1.11. It is speculated that the nonlinear response was caused by an increase in electron confinement and the resultant buildup of orbiting electrons due to the negative potential on all of the electrodes surrounding the electron orbiting volume. Evidence leading to this speculation included the fact that at a fixed pressure the sensitivity of the SGOG would increase by as much as a factor of two during a period of ~ 1 hr. When the filament was de-energized the gauge continued to operate for as much as 20 to 30 min. before the ion collector current would fall to its normal background current level. Upon reactivation of the filament the gauge would indicate the original sensitivity level and begin the sensitivity buildup again.

When the SGOG was mounted on the uhv pressure-ratio system it was determined that a linear response could be achieved if the negative potential applied to the cathode and reflector tubes was reduced. The negative background current at the ion collector decreased from ~ -1 x 10^{-11} A to ~ -1 x 10^{-12} A when this potential was changed from -100 V to -19 V.

B. Conclusions

The following conclusions can be drawn from the above data:

1. Nude orbitron gauges of several designs have been used as reliable linear pressure transducers over a wide range of pressures.

2. The reduced area ion collector concept does result in low background currents at the 1 µA emission current level, however the background current to ion current ratio is not improved. At an emission current of 7 µA the sensitivity is 0.034 A/torr N_2, however, the background currents still limit the gauge usefulness in the ultra low pressure range.

3. The combination of the suppressor grid technique with the orbitron gauging technique displays superior performance. The response of the SGOG

indicates that with improved high voltage power supplies and a proper adjustment of parameters this type of gauge may be useful through the 10^{-12} torr range.

4. The response, linear and nonlinear, of the SGOG as a function of the operating parameters has provided a useful insight into the condition for confinement of electrons within the electron orbiting volume. Under the proper condition it may be possible to establish a reasonably stable saturated space change condition. It is interesting to speculate that in devices other than gauges (such as pumps) which incorporate orbiting electron techniques a significant improvement in discharge activity (resulting in higher pump speeds) may be obtained if the electron confining electrodes are the most negative surfaces within the device.

V. RESPONSE OF BURIED COLLECTOR GAUGE

The low pressure ion current response characteristics for a buried collector gauge has been determined via the uhv pressure ratio comparison technique.

The buried collector gauge used in this study was modified from the original gauge supplied by NASA (Langley Research Center). The tungsten ribbon filament was replaced by a thoria-coated ribbon filament. Also, the orientation of the filament plane was changed from tangential to normal with reference to the grid.

Four sets of data are presented in Figure 19, i.e., two sets of pressure ratio comparisons to a B-A gauge, and two sets of direct comparison to a B-A gauge. Both reference B-A gauges were calibrated through the 10^{-8} torr range via a pressure reference transfer technique (ref. 13) and through the 10^{-9} torr range via the pressure ratio technique. Although the test gas used was helium, the data shown in Figure 19 have been presented in torr nitrogen equivalent units.

A background collector current of 6 to 9 x 10^{-13} A was measured in the 10^{-13} torr range. As pressure is increased the collector current response approaches a linear response curve with a slope of 0.05 A/torr N_2. This response was obtained with the following parameters:

Filament	+300 V
Focusing ring	+300 V
Grid	+450 V
Collector	0 V
Emission	0.004 A

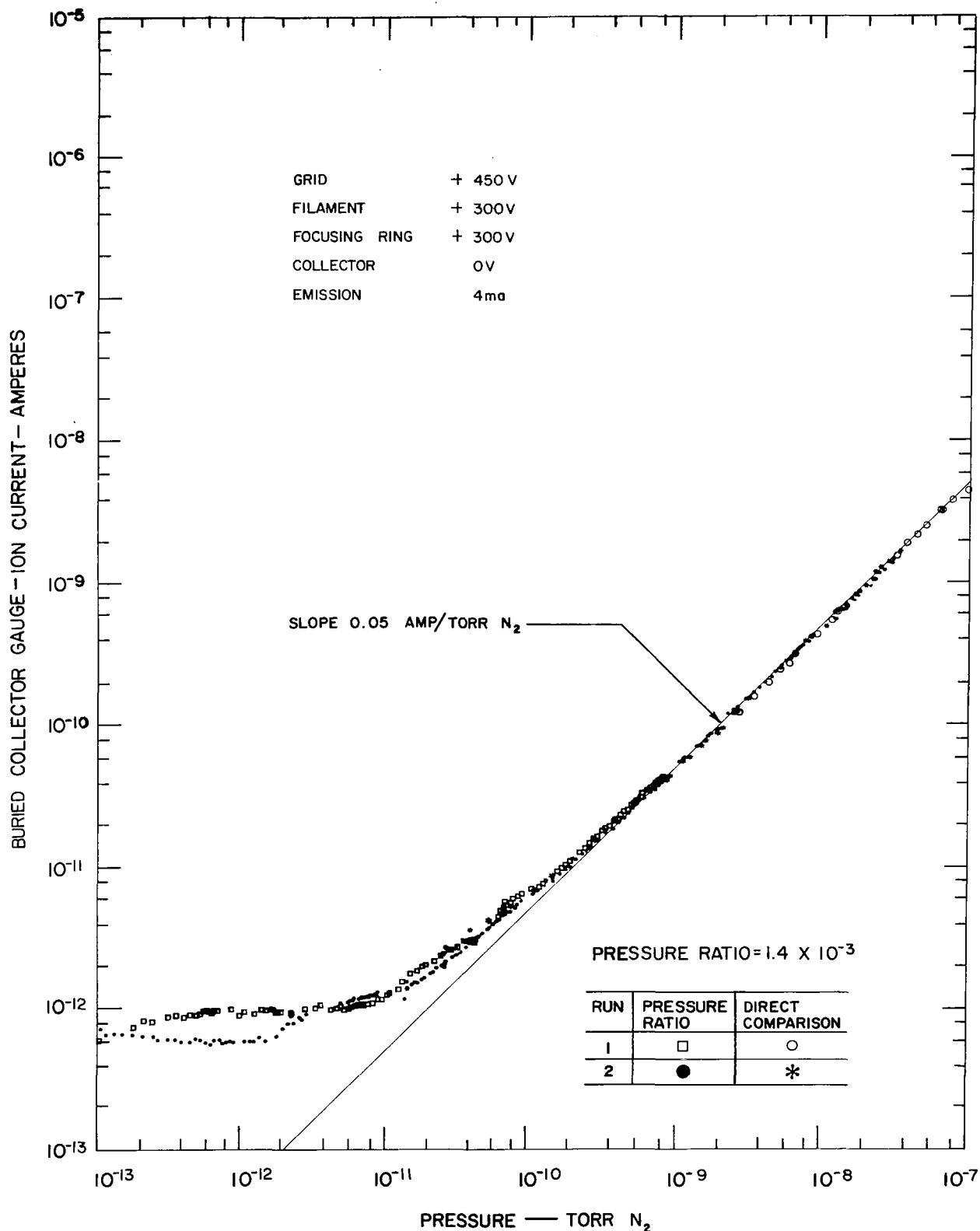The gauge constant for nitrogen was therefore 12.5 torr^{-1}.

Figure 19 - Low Pressure Current Response Characteristic for a Buried Collector Gauge. Four sets of data are presented in torr N_2 equivalent units. Two sets were obtained by the pressure ratio comparison technique and two sets by the direct comparison technique. The gauge response approached a linear curve of slope 0.05 A/torr N_2 as pressure was increased.

Effects of focusing ring voltage were studied briefly at two pressures, i.e., $\sim 1 \times 10^{-10}$ torr and $\sim 3 \times 10^{-8}$ torr. It was found that at 1×10^{-10} torr the collector current was increased approximately an order of magnitude by increasing the focusing ring voltage from 300 V to 400 V. The collector current reached a maximum at about 430 V and then decreased sharply. At $\sim 3 \times 10^{-8}$ torr there was less than 10% increase or decrease in collector current as the focusing ring voltage was varied from +300 to +390 V. Above +390 there was a rapid decrease in collector current. The fall-off of collector current at high voltage at both pressures can be interpreted as a serious reduction in the focusing of ions onto the collector; however, the difference between the collector current response at the two pressure levels below 390 V indicates the presence of significant amounts of ionizable adsorbed gas on the focusing ring. Although the gauge was degassed prior to the studies, the effect was still observed. The basic degassing problem, however, is the amount of power needed to clean the focusing ring. In one degassing operation the grid was damaged and had to be replaced.

Reducing the voltage on the focusing ring would aid in reducing surface generated ions; however, in the 3×10^{-8} torr study, the collector current response indicates a decreasing gauge sensitivity as the voltage was reduced below +300 V.

The above data indicate that a reduced area focusing ring should reduce the background in the buried collector gauge.

REFERENCES

1. D. Lichtman, *J. of Vac. Sci. & Tech.*, 2, p. 70 (1965).

2. R. T. Bayard and D. Alpert, *Rev. Sci. Inst.*, 21, 571 (1950).

3. W. C. Schuemann, *Trans. 9th Nat. Vac. Symp.*, 1962, 428, MacMillan Co., New York, also see *Rev. Sci. Inst.*, 34, 700 (1963).

4. W. G. Mourad, T. Pauly, and R. G. Herb, *Rev. Sci. Inst.*, 35, 661 (1964).

5. F. P. Clay, Jr., and L. T. Melfi, Jr., *J. Vac. Sci & Tech.*, 3, 167 (1966).

6. M. Knudsen, *Ann. Physik*, 28, 76 and 999 (1909); 29, 179 (1909); 31, 633 (1910); 44, 525 (1914).

7. N. A. Florescu, *Trans. Natl. Vac. Symp.*, 1961, 504 (1962).

8. J. R. Roehrig and J. C. Simons, Jr., *Trans. Natl. Vac. Symp.*, 1961, 511.

9. S. Dushman and C. G. Found, *Phys. Rev.*, 17, 7 (1921).

10. R. E. Honig, *J. Appl. Phys.*, 16, 646 (1945).

11. P. J. Bryant, C. M. Gosselin, and W. W. Longley, Jr., *Jour. Vac. Sci. and Tech.*, 3, 62 (1966), also, NASA Contractor Reports NASA CR-324 (1965) and NASA CR-7206 (1967).

12. P. J. Bryant and C. M. Gosselin, *Jour. Vac. Sci. and Tech.*, 3, 350 (1966).

13. C. F. Morrison, *J. Vac. Sci. & Tech.*, 4, 246 (1967).

14. P. J. Bryant and C. M. Gosselin, NASA Contractor Report, NASA CR-886 (1967).